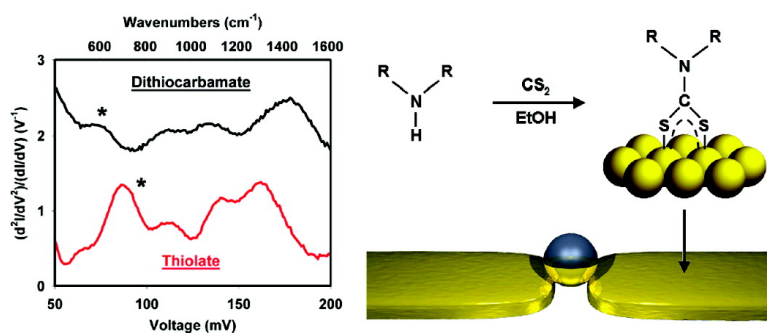


Inelastic Electron Tunneling Spectroscopy of Alkane Monolayers with Dissimilar Attachment Chemistry to Gold

David P. Long, and Alessandro Troisi

J. Am. Chem. Soc., **2007**, 129 (49), 15303-15310 • DOI: 10.1021/ja074970z

Downloaded from <http://pubs.acs.org> on February 9, 2009



More About This Article

Additional resources and features associated with this article are available within the HTML version:

- Supporting Information
- Access to high resolution figures
- Links to articles and content related to this article
- Copyright permission to reproduce figures and/or text from this article

[View the Full Text HTML](#)

Inelastic Electron Tunneling Spectroscopy of Alkane Monolayers with Dissimilar Attachment Chemistry to Gold

David P. Long^{*,†} and Alessandro Troisi[‡]

Contribution from the Research and Development Center, Science Applications International Corporation (SAIC), 9460 Innovation Drive, Manassas, Virginia 20110, and Department of Chemistry and Centre of Scientific Computing, University of Warwick, Gibbet Hill Road, CV4 7AL Coventry, U.K.

Received July 24, 2007; E-mail: longdp@saic.com

Abstract: We compare the low-temperature electron transport properties of alkyl monolayers which utilize different attachment strategies to gold. Inelastic electron tunneling spectroscopy (IETS) and current–voltage analysis were performed on molecular junctions incorporating alkyl-dithiocarbamate and alkanethiolate self-assembled monolayers of similar length. Alkyl-dithiocarbamate monolayers were formed by the condensation of dioctylamine or didecylamine with carbon disulfide in anhydrous ethanol and compared to alkanethiolate SAMs of 1-decanethiol and 1-dodecanethiol, respectively. The electron transport properties of each monolayer were examined using magnetically assembled microsphere junctions under high-vacuum conditions at low temperature. IETS was employed to differentiate the films on the basis of vibrational modes which are characteristic of each method of attachment. We use quantum chemical simulations of model compounds to calculate frequency and intensity of predicted signals arising from molecular vibrations to aid in the accurate assignment of the spectra. A qualitative comparison of our devices also reveals an increase in current density when utilizing dithiocarbamate attachment to gold compared to alkanethiolate molecules of similar length.

Introduction

The chemisorption of thiols on gold remains the most widely used technique for creating self-assembled monolayers (SAMs) and metal–molecule contacts in the fabrication of molecular junctions.^{1,2} This virtual monopoly is due to the simplicity and great versatility provided by gold–thiol SAM formation.³ Although convenient for monolayer deposition, thiols are known to undergo undesirable reactions, such as displacement from the metal surface, which can lead to degradation of film quality and packing structure.^{4,5} Thiolate attachment to gold has also been shown to yield relatively poor electronic coupling between a molecule and the electrode, increasing the resistance to electron transport through the metal–molecule interface.⁶ A potential solution to these problems is the utilization of alternate attachment strategies which can function as nanoscale “alligator clips” to metal surfaces in order to improve performance in molecular junctions.^{6–9} One promising alternative is the self-

assembly of molecular dithiocarbamates (DTC) on gold.^{10,11} Although still dependent on the formation of gold–sulfur contacts, DTC monolayers have been shown to exhibit improved physical, chemical, optical, and electronic properties which could be beneficial for the fabrication of molecular electronics.^{11–15} Of particular interest is the bidentate structure of the dithiocarbamate moiety (N–C–S₂) whose delocalized orbitals and π -conjugation are predicted to increase electronic coupling to surface metal binding sites and enhance charge transport through the molecule.¹⁵ In addition, the interatomic distance between the terminal sulfur atoms of the DTC group is consistent with the atomic spacing found on Au(111) surfaces and nearly ideal for epitaxial adsorption of the molecule.^{3,16} The bidentate structure adopted by the DTC moiety could also give rise to a stabilizing “chelate effect”, resulting in a more robust monolayer for improved junction performance.¹⁶ Also, a simple approach

[†] Science Applications International Corporation (SAIC).

[‡] University of Warwick.

- (1) Love, J. C.; Estroff, L. A.; Kriebel, J. K.; Nuzzo, R. G.; Whitesides, G. M. *Chem. Rev.* **2005**, *105*, 1103–1169.
- (2) James, D. K.; Tour, J. M. *Chem. Mater.* **2004**, *16*, 4423–4435.
- (3) Ulman, A. *Chem. Rev.* **1996**, *96*, 1533–1554.
- (4) Schlenoff, J. B.; Li, M.; Ly, H. *J. Am. Chem. Soc.* **1995**, *117*, 12528–12536.
- (5) Flynn, N. T.; Tran, T. N.; Cima, M. J.; Langer, R. *Langmuir* **2003**, *19*, 10909–10915.
- (6) Lang, N. D.; Kagan, C. R. *Nano Lett.* **2006**, *6*, 2955–2958.
- (7) Bai, P.; Li, E.; Neerja Collier, P. *IEEE Trans. Nanotechnol.* **2005**, *4*, 422–429.
- (8) Kushmerick, J. G.; Whitaker, C. M.; Pollack, S. K.; Schull, T. L.; Shashidhar, R. *Nanotechnology* **2004**, *15*, S489–S493.

- (9) Tulevski, G. S.; Myers, M. B.; Hybertsen, M. S.; Steigerwald, M. L.; Nuckolls, C. *Science* **2005**, *309*, 591–594.
- (10) Thorn, G. D.; Ludwig, R. A. *The Dithiocarbamates and Related Compounds*; Elsevier: Amsterdam, 1962.
- (11) Zhao, Y.; Segarra, W. P.; Shi, Q.; Wei, A. *J. Am. Chem. Soc.* **2005**, *127*, 7328–7329.
- (12) Morf, P.; Raimondi, F.; Nothofer, H.-G.; Schnyder, B.; Yasuda, A.; Wessels, J. M.; and Jung, T. A. *Langmuir* **2006**, *22*, 658–663.
- (13) Hill, J. O.; Magee, R. *J. Rev. Inorg. Chem.* **1981**, *3*, 141–197.
- (14) Wessels, J. M.; Nothofer, H.-G.; Ford, W. E.; von Wrochem, F.; Scholz, F.; Vossmeier, T.; Schroedter, A.; Weller, H.; Yasuda, A. *J. Am. Chem. Soc.* **2004**, *126*, 3349–3356.
- (15) Li, Z.; Kosov, D. S. *J. Phys. Chem. B* **2006**, *110*, 9893–9898.
- (16) Colorado, R., Jr.; Villazana, R. J.; Lee, T. R. *Langmuir* **1998**, *14*, 6337–6340.
- (17) Querner, C.; Reiss, P.; Bleuse, J.; Pron, A. *J. Am. Chem. Soc.* **2004**, *126*, 11574–11582.

recently reported which describes the spontaneous self-assembly of dithiocarbamate molecules on gold from a wide variety of secondary amines suggests that the diversity of DTC ligands available for monolayer formation may rival that provided by thiols.¹¹

The introduction of novel attachment strategies in molecular electronics will require extensive electrical characterization in order to determine the inherent properties of each new system. Here we report the fabrication and low-temperature electron transport analysis of molecular junctions which differ by the chemical attachment of the incorporated monolayers to gold. Inelastic electron tunneling spectroscopy (IETS) and current–voltage $I(V)$ analysis are used to characterize alkyl monolayers which employ dithiocarbamate and thiolate surface attachments. IETS has recently evolved into an important nanoscopic tool for determining the interactions between tunneling electrons and discrete molecular vibrations within a junction.^{18–21} Beyond the simple identification of incorporated molecules within a device, IETS can yield valuable information on molecular geometry, chemical environment, the influence of the metal contacts, and the pathway electrons follow through a molecule.^{22–25} Thus, a comparison of different chemical attachments to metal surfaces using IETS could improve our understanding of charge transport in molecular junctions which incorporate increasingly complex organic systems. Our technique to acquire IETS uses magnetically assembled microsphere junctions combined with standard ac modulation techniques as previously described.^{23,26} DTC monolayers were formed by the condensation of secondary alkylamines with carbon disulfide (1:1) in the presence of gold-coated magnetic arrays as shown in Figure 1. Monolayers of dioctylamine (DOA) DTC were compared with those of 1-decanethiol (C-10), while SAMs of didecylamine (DDA) DTC were compared to those of 1-dodecanethiol (C-12). These molecules were chosen since they incorporate an identical number of chemical bonds from the terminal CH_3 group of the SAM to the sulfur–gold contacts and could be used to compare the relative conductivity of the different monolayer systems.

Experimental Section

Chemicals. Anhydrous ethanol (200 proof), 30% hydrogen peroxide (in water), carbon disulfide (99%), dioctylamine (98%), didecylamine (98%), 1-decanethiol (96%), and 1-dodecanethiol (98%) were all purchased from Aldrich and used as received.

Substrate Preparation and SAM Deposition. Magnetic arrays composed of evaporated gold-coated nickel features and incorporating a $0.5 \mu\text{m}$ spacing between the source/drain electrodes were cleaned using sonication in anhydrous ethanol for 10 min, followed by air-drying and immersion for 30 min in 30% hydrogen peroxide solution.

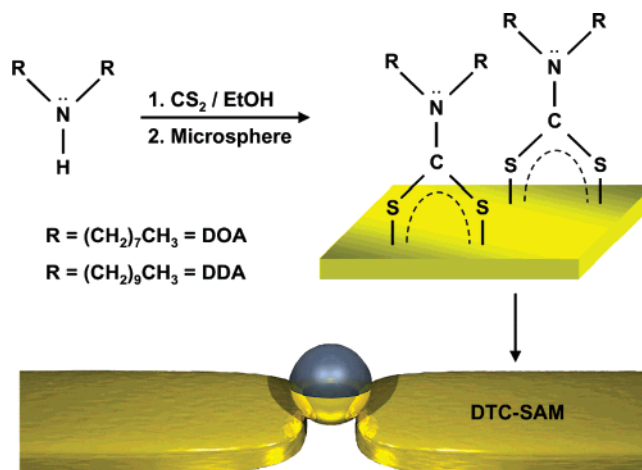


Figure 1. Illustration showing the formation of a dithiocarbamate (DTC) self-assembled monolayer on a gold-coated magnetic array using a 1:1 mixture of secondary alkylamine and carbon disulfide in anhydrous ethanol.¹¹ Top electrical contact to the SAM is formed by depositing magnetic colloid into the gap. Details for the fabrication of microsphere junctions have been described previously.^{23,26}

Arrays were then rinsed with additional anhydrous ethanol and again sonicated for 20 min in fresh solvent. Substrates were dried using nitrogen gas and exposed to argon plasma for 5 min (Plasma Prep II SPI Supplies, West Chester, PA). Cleaned magnetic arrays were immediately transferred to freshly prepared anhydrous ethanol solutions of the molecule being deposited. For alkyl-dithiocarbamate monolayers, $100 \mu\text{L}$ of CS_2 was added to 1 mL of anhydrous ethanol and briefly sonicated. Then 0.400 g of dioctylamine (1.66 mM) was dissolved into 3 mL of anhydrous ethanol with sonication. The ethanol solution containing the amine was added slowly to the CS_2 solution and sonicated for 5 min. After mixing, the solution takes on a faint yellow color. Into this prepared mixture is placed our gold-coated nickel arrays. The substrate was allowed to remain immersed overnight (approximately 20 h) during which time the color of the solution becomes intensely yellow in color but remains free of precipitate. Arrays were then removed, rinsed well with additional solvent, and sonicated for 60 s before being dried under a stream of nitrogen. Formation of didecylamine dithiocarbamate SAMs were performed using a similar procedure at identical molar concentrations. Deposition of 1-decanethiol and 1-dodecanethiol were performed using $2 \mu\text{L}$ of the thiol dissolved in 10 mL of anhydrous ethanol. This solution was briefly sonicated before adding the cleaned magnetic arrays for approximately 20 h followed by rinsing and 60 s of sonication in fresh solvent.

Fabrication of Microsphere Junctions. The fabrication of metalized silica colloid dispersed in anhydrous ethanol has been described previously.²⁶ This “stock” solution was further diluted by dispersing 0.3 mL into 100 mL of anhydrous ethanol followed by sonication for 30 min. Approximately 10 mL of this diluted solution was used for each microsphere deposition onto the arrays. Magnetic assembly was performed in a test tube by immersing the SAM-functionalized magnetic array in the colloid solution for 25 min under an external 225 G magnetic field oriented parallel with the long axis of the features in the array. After assembly, devices were dried under nitrogen and transferred to a low-temperature vacuum probe station for electrical analysis.

Electrical Analysis. Current–voltage analysis of fabricated devices was performed under dynamic vacuum (1×10^{-6} Torr) in a Desert Cryogenics vacuum probe station fitted with an Agilent 4155A parametric analyzer under computer control. $I(V)$ analysis was performed from $\pm 200 \text{ mV}$ bias at both room temperature and after cooling devices to $5\text{--}7 \text{ K}$ using liquid helium. IETS was acquired on fabricated microsphere junctions using standard ac modulation techniques and dual lock-in amplifiers to simultaneously record the current–voltage

- (18) Yu, L. H.; Zangmeister, C. D.; Kushmerick, J. G. *Nano Lett.* **2006**, *6*, 2515–2519.
- (19) Cai, L.; Cabassi, M. A.; Yoon, H.; Cabarcos, O. M.; McGuinness, C. L.; Flatt, A. K.; Allara, D. L.; Tour, J. M.; Mayer, T. S. *Nano Lett.* **2005**, *5*, 2365–2372.
- (20) Kushmerick, J. G.; Lazorcik, J. L.; Patterson, C. H.; Shashidhar, R.; Seferos, D. S.; Bazan, G. C. *Nano Lett.* **2004**, *4*, 639–642.
- (21) Wang, W.; Lee, T.; Kretzschmar, I.; Reed, M. A. *Nano Lett.* **2004**, *4*, 643–646.
- (22) Troisi, A.; Ratner, M. A. *Small* **2006**, *2*, 172–181.
- (23) Long, D. P.; Lazorcik, J. L.; Mantooth, B. A.; Moore, M. H.; Ratner, M. A.; Troisi, A.; Yao, Y.; Ciszek, J. W.; Tour, J. M.; Shashidhar, R. *Nat. Mater.* **2006**, *5*, 901–908.
- (24) Troisi, A.; Beebe, J. M.; Picraux, L. B.; van Zee, R. D.; Stewart, D. R.; Ratner, M. A.; Kushmerick, J. G. *Proc. Natl. Acad. Sci. U.S.A.* **2007**, *104*, 14255–14259.
- (25) Troisi, A.; Ratner, M. A. *Phys. Chem. Chem. Phys.* **2007**, *9*, 2421–2427.
- (26) Long, D. P.; Patterson, C. H.; Moore, M. H.; Seferos, D. S.; Bazan, G. C.; Kushmerick, J. G. *Appl. Phys. Lett.* **2005**, *86*, 153105.

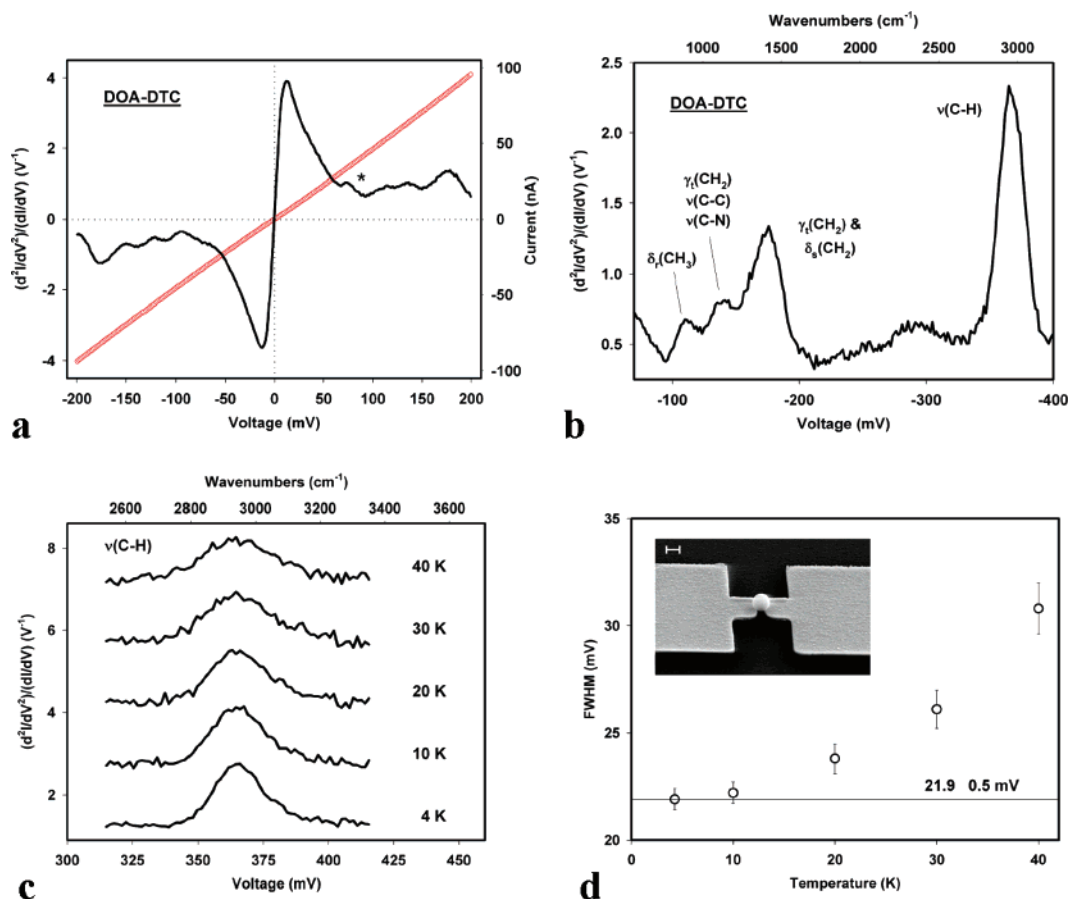


Figure 2. (a) DOA-DTC IETS and $I(V)$ characteristics from ± 200 mV bias. Asterisk marks the peak associated with the dithiocarbamate ($\text{N}-\text{C}-\text{S}_2$) moiety. (b) IETS showing the dominant alkyl modes from a DOA-DTC microsphere junction. All IET spectra were acquired using a 6 mV modulation voltage and plotted as d^2I/dV^2 normalized by the differential conductance (dI/dV). (c) Broadening of the $\nu(\text{C}-\text{H})$ stretching mode (365 mV, 2944 cm^{-1}) as a result of increasing temperature. (d) Plot showing IETS line width as a function of temperature. (Inset) SEM of a microsphere junction, scale bar = 1 μm .

characteristics and the first and second harmonics (proportional to dI/dV and d^2I/dV^2 , respectively). IETS parameters were optimized for individual junctions in order to accommodate changing current levels and device quality. Typical instrument settings were as follows: temperature (5–7 K), lock-in time constant (1 s), ac modulation voltage (4–6 mV), step size (1–2 mV). Before each data point is acquired a delay of 2–4 s is applied to allow the lock-in amplifier to stabilize. Each data point is the average of 2000–4000 samples with a delay of ~ 1 ms between each.

Computational Details. The protocol described in ref 27 was followed here. Specific to this article are the clusters used to compute the metal–molecule coupling. Three and four gold atoms have been considered for the interaction between the thiolate and dithiocarbamate functionalities and the gold surface. Four gold atoms are used for the interaction between the methyl-terminated groups of C-10. Two groups of four atoms have been used to simulate the coupling between the alkylic portion of the DTC and the gold surface. The molecules were kept perpendicular to the electrode surface, and the sulfur–gold distance was optimized, in both cases, under this constraint. According to a recent study, the effect of tilting the molecular orientation can alter the relative importance of some signals but does not affect the basic assignment of the IETS spectrum.²⁵ All the computations (optimizations and frequency analysis) are at the B3LYP level of theory with the 6-31G* basis set used for the molecule and the LanL2mb basis set/pseudopotential used for the gold atoms. The DTC cluster had total net charge of -1 , while the alkanethiolate cluster was neutral. The computed frequency modes have been scaled by the recommended factor 0.961. The intensities derived from the computational study are

reported in Tables 1 and 2 in the Supporting Information. The Gaussian broadening introduced to facilitate a direct comparison with experimentally obtained spectra was 40 cm^{-1} in Figure 4a and 80 cm^{-1} in Figure 4b.

Results and Discussion

Figure 2 displays the low-temperature electron transport data for a DOA-DTC microsphere junction. An IET “survey” spectrum, including the device $I(V)$ characteristics, is shown in Figure 2a. The current–voltage properties for the device are found to be linear over this bias range while a plot of d^2I/dV^2 shows several features originating from molecular vibrations within the monolayer. The inverted symmetry apparent in the spectrum, with molecular vibrations displaying equal intensity in both bias polarities, is also consistent with a molecular origin to the acquired signal. The small peak observed at 71 mV (see asterisk) originates from the dithiocarbamate functional group ($\text{N}-\text{C}-\text{S}_2$) and is discussed in detail below. Figure 2b shows IETS from 70 to 400 mV of the same DOA-DTC junction. The alkyl-dithiocarbamate spectrum displays a clear similarity to previous IETS obtained on a C-11 alkanethiolate SAM using a crossed-wire tunnel junction.²⁰ The similarity to prior alkanethiolate spectra suggests that vibronic coupling in DTC monolayers also favors longitudinal modes parallel with the molecular structure and dominated by interactions with the hydrocarbon substituents. A prominent peak associated with $\nu(\text{C}-\text{H})$ stretching vibrations is visible at 365 mV, while several overlapping peaks due to C–H bending and $\nu(\text{C}-\text{C})$ and $\nu(\text{C}-\text{N})$ stretching

(27) Troisi, A.; Ratner, M. A. *J. Chem. Phys.* **2006**, *125*, 214709.

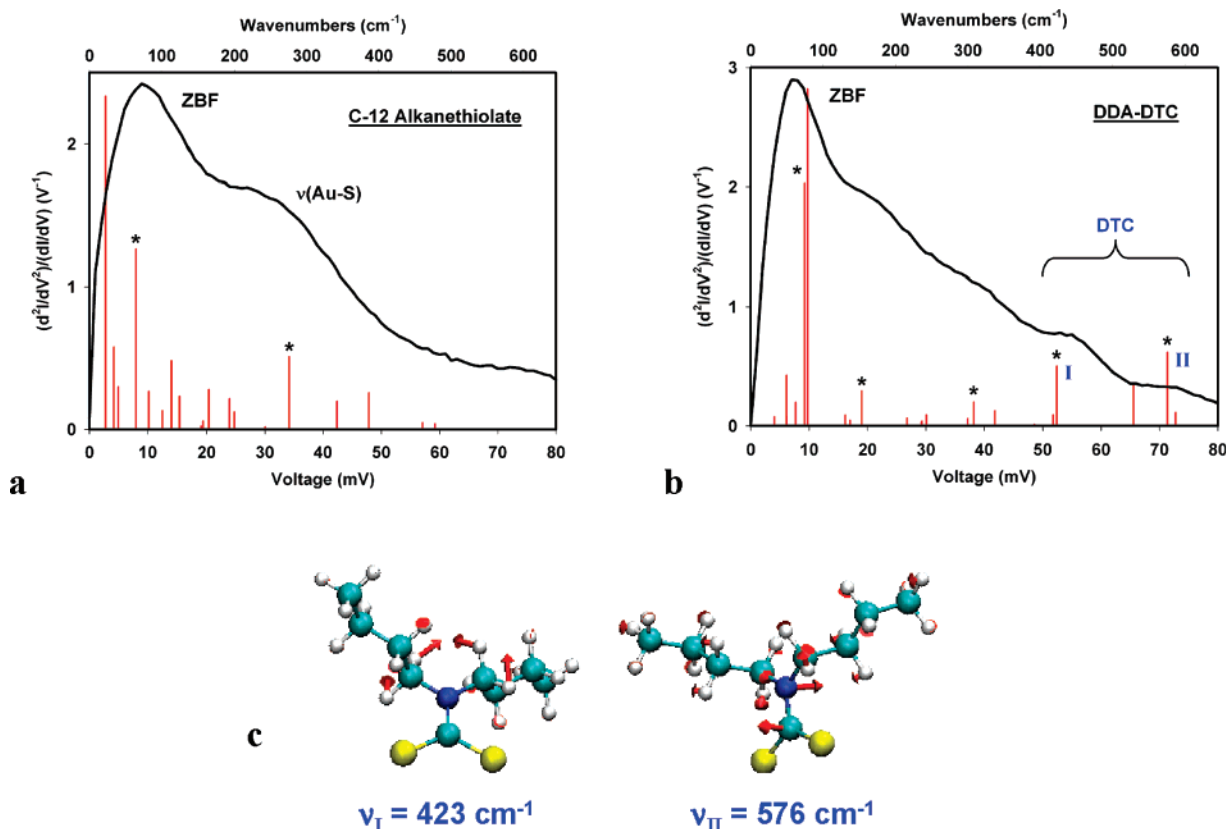


Figure 3. Comparison of (a) alkanethiolate and (b) alkyl-dithiocarbamate experimental IETS from 0 to 80 mV bias. Both spectra acquired using a 4 mV ac modulation voltage at 7 K. Red sticks represent calculated vibrational modes with heights proportional to predicted IETS intensity. Asterisks mark calculated modes which coincide with dominant peaks observed in the experimental spectra. (c) Characteristic molecular vibrations of the dithiocarbamate moiety (N–C–S₂) using the model system. Modes I (423 cm⁻¹) and II (576 cm⁻¹) are labeled in b at their predicted locations.

modes are found between 100 mV and 200 mV. The weak signal centered at 292 mV (2355 cm⁻¹) arises from trace amounts of water in the monolayer.²³ We attribute the increased intensity of this peak relative to alkanethiolate monolayers maintained under similar anhydrous conditions to the negative charge on the DTC moiety which would promote stronger binding of water molecules in the SAM. IETS of alkyl-DTC microsphere junctions yield $\nu(\text{C-H})$ stretching modes with fwhm of 21.9 mV \pm 0.5 mV at 4.2 K and 6 mV modulation voltage, placing DTC IET line width within the range determined previously for alkanethiolate monolayers using identical procedures.²³ The similar IETS characteristics displayed by alkyl-dithiocarbamate monolayers compared to those of previous alkanethiolate SAMs suggests electron transport in both systems takes place through an identical mechanism and is modulated by the alkyl substituents.

To confirm our DTC spectra are truly the result of inelastic tunneling within our devices, we performed a variable-temperature control experiment in order to measure the rate of peak broadening as a function of temperature.²³ Thermal broadening is a fundamental property of inelastic electron tunneling and is a particularly sensitive test to verify the recorded second harmonic signal (d^2I/dV^2) is solely the result of this mechanism.^{28,29} IETS was acquired from 4.2 to 40 K using a constant modulation voltage of 6 mV. The series of scans shown in Figure 2c were performed from 315 to 415 mV in order to record the prominent $\nu(\text{C-H})$ stretching mode for analysis. A

Gaussian function was then used to fit the experimental IETS data to determine the fwhm of each peak and plotted as a function of temperature (Figure 2d). Linear regression was employed to determine the slope of the resulting line which was compared to the theoretical value calculated from finite temperature (4.2 K) and voltage modulation (6 mV) effects.²⁸ The rate of thermal broadening determined in our control experiment ($b = 0.35_{\text{exp}}$) matched the theoretical value ($b = 0.375_{\text{theoretical}}$), confirming that our spectra arise from IET processes within the monolayer, thus validating our spectra as genuine and molecular in origin.

In order to differentiate molecular junctions incorporating alkyl-dithiocarbamate and alkanethiolate monolayers, and to confirm electron transport through the DTC moiety, we performed a detailed IETS comparison of C-12 and DDA-DTC SAMs at low voltage, the results of which are shown in Figure 3. All vibrational modes discussed are listed in Table 1. The assignment of the IETS signatures to specific molecular vibrations was aided by the comparison with quantum chemical simulations based on the theoretical model described in references 30 and 31 and tested recently on several relevant systems.^{23,25} These and analogous models have proven very useful for the interpretation of IET spectra and provide a means to translate the data into chemically relevant information.^{32–36}

(30) Troisi, A.; Ratner M. A.; Nitzan, A. *J. Chem. Phys.* **2003**, *118*, 6072–6082.

(31) Troisi, A.; Ratner M. A. *Phys. Rev. B* **2005**, *72*, 033408.

(32) Paulsson, M.; Frederiksen, T.; Brandbyge, M. *Nano Lett.* **2006**, *6*, 258–262.

(33) Solomon, G. C.; Gagliardi, A.; Pecchia, A.; Frauenheim, T.; Carlo, A. D.; Reimers, J. R.; Hush, N. S. *J. Chem. Phys.* **2006**, *124*, 094704.

(28) Wang, W.; Lee, T.; Reed, M. A. *Proc. IEEE* **2005**, *93*, 1815–1824.

(29) Lambe, J.; Jaklevic, R. C. *Phys. Rev.* **1968**, *165*, 821–832.

Table 1. Summary of Alkyl-dithiocarbamate and Alkanethiolate Vibrational Modes Discussed in Text

molecular attachment	observed frequencies			mode
	experimental	calculated		
	(mV)	(mV)	(cm ⁻¹)	
alkyl-dithiocarbamate	19 ^a	19.0	153.49	C–C–C bending ^b
	37 ^a	38.2	308.07	CH ₂ twisting and CCC bending ^b
	53 ^a	52.4	422.73	CH ₂ rocking (adjacent to N)
	–	65.6	528.89	C–N _{oop} and CH ₂ rocking
	71 ^a	71.4	575.64	C–N _{oop}
	–	94.6	763.06	CH ₂ rocking
	–	95.5	770.44	CH ₂ rocking
	111	110.8	893.62	ν_s (N–CH ₂) and C–H rocking
	–	135.0	1088.86	ν (C=N) and CH ₂ twisting
	134	135.6	1093.90	CH ₂ twisting and ν (C=N)
	–	135.9	1096.07	ν (C–C) and CH ₂ wagging
	–	162.4	1309.97	CH ₂ twisting adjacent to DTC
	164 ^a	167.7	1352.62	CH ₂ twisting adjacent to DTC
	176	176.7	1425.00	CH ₂ scissoring
–	180.6	1456.57	CH ₂ scissoring	
365	368.1	2968.78	ν (C–H)	
alkanethiolate	20–40 ^a	34.2	275.81	ν (Au–S), CCC bending
	87	88.0	710.21	ν (S–C)
	111	103.9	838.35	ν (C ₁ –C ₂)
	–	126.2	1017.78	ν (C–C)
	140	137.2	1107.03	ν (C–C)
	–	155.7	1256.02	CH ₂ wagging
	162	163.9	1322.35	CH ₂ wagging
	–	172.0	1387.13	CH ₃ bending
	364	362.4	2923.33	ν (C–H)

^a Modes observed as shoulder peaks in experimentally obtained spectra, location approximate. ^b Assignment tentative.

A quantum chemical computation including the molecule and several electrode atoms was used to evaluate the molecule–metal coupling, while the vibrational frequencies derives from a gas-phase quantum chemical computation at the B3LYP/6-31G* level.²⁷ Calculated vibrational modes are displayed beneath each spectrum at their predicted frequency with heights proportional to the computed IETS intensity. The computations provide frequency and intensity of the IETS signals arising from molecular vibrations (additional details are given in the Experimental Section and Supporting Information). The dibutyl-dithiocarbamate molecule which incorporates shorter alkyl substituents was used as a model compound to aid in interpretation of DTC experimental spectra.

The spectra presented in Figure 3 differ extensively in the pattern of vibrational modes which appear as shoulders on the zero bias features (ZBF). IETS acquired on a C-12 SAM (Figure 3a) displays a prominent ZBF whose maximum intensity occurs at 9 mV. The physical origin of this peak is still debated but has been associated with non-molecular phonon interactions in the electrode.^{37,38} Our computation also predicts intense signals in this region due to large amplitude motions of the alkyl

portions of both molecules. However, these low-frequency modes are likely coupled to intermolecular motions of the monolayer (ignored by the computation) and appear to carry little information on chemical details at the interface. In addition to the ZBF in Figure 3a, the most prominent feature in this voltage range is a single broad shoulder centered at approximately 27 mV (218 cm⁻¹). The intensity and width of this feature is due to multiple low-frequency ν (Au–S) stretching modes arising from different adsorption sites on the electrode surface with additional contributions from large amplitude C–C–C and C–C–S deformations.^{32–35,39} All IET spectra recorded on alkanethiolate SAMs using the microsphere test-bed, irrespective of hydrocarbon chain length, contain a single broad shoulder similar to the one shown here. IETS of DDA-dithiocarbamate monolayers show a different pattern of vibrational modes from 0 to 80 mV and distinct from those of the C-12 SAM (Figure 3b). The largest- and lowest-energy peak of the ZBF is found at a similar voltage compared to that of the C-12 spectrum, as expected for the non-molecular origin of this signal. However, four distinct shoulder peaks are apparent from 20 to 80 mV which we only observe in DTC monolayers. The two shoulders found on the ZBF at approximately 53 mV (427 cm⁻¹) and 71 mV (573 cm⁻¹) are clearly predicted by our simulation and can be confidently assigned to specific vibrations of the DTC functional group. The most prominent of these modes at 53 mV (I) and illustrated in Figure 3c, derives from a rocking motion of the CH₂ groups directly adjacent to the nitrogen atom of the DTC moiety. The remaining peak centered at 71 mV coincides with an out-of-plane (oop) motion of the carbon and nitrogen atoms of the delocalized N–C–S₂ moiety. (Video clips of these molecular vibrations are provided in the Supporting Information) These modes have the common characteristic of mixing π -orbitals found on the delocalized DTC group with σ -orbitals of the alkyl substituents. The σ – π mixing modes are IETS active in junctions containing a combination of saturated and conjugated molecular segments.²⁴ The appearance of these distinct DTC modes confirms electron transport through the delocalized bonds of the dithiocarbamate attachment. Recent analysis of DDA-DTC monolayers using surface-enhanced Raman spectroscopy (SERS) also shows intense vibrations which coincide in frequency with these peaks.¹¹ Comparing the computed Raman and our IETS results, we observed that the IETS signal at 53 mV is due to the same normal mode causing the strong SERS signal, while the IETS signal at 71 mV originates from a different (slightly lower-energy) mode than the one responsible for the SERS peak. This example underscores that comparison with Raman spectroscopy can be helpful but not conclusive for the interpretation of IETS spectra since the two spectroscopic techniques obey different sets of propensity rules.

The remaining low-energy shoulders at approximately 19 and 37 mV in Figure 3b lie in the ν (Au–S) stretching region of the IET spectrum and appear centered on the frequency which coincides with the single broad mode observed in alkanethiolate SAMs at 27 mV. The appearance of these peaks is consistent with gold–sulfur stretching vibrations which have split into two modes representing the fundamental symmetric ν_s (Au–S) and asymmetric ν_{as} (Au–S) motions expected for bis-chelated DTC

- (34) (a) Jiang, J.; Kula, M.; Lu, W.; Luo, Y. *Nano Lett.* **2005**, *5*, 1551–1555.
 (b) Kula, M.; Jiang, J.; Luo, Y.; *Nano Lett.* **2006**, *6*, 1693–1698.
 (35) Galperin, M.; Ratner, M. A.; Nitzan, A. *J. Chem. Phys.* **2004**, *121*, 11965–11979.
 (36) Seminario, J. M.; Cordova, L. E. *J. Phys. Chem. A* **2004**, *108*, 5142–5144.
 (37) Weber, H. B.; Häußler, R.; von Löhneysen, H.; Kroha, J. *Phys. Rev. B* **2001**, *63*, 165426.

- (38) Agnolet, G.; Savitski, S. R.; Zimmerman, D. T. *Phys. B* **2000**, 284–288, 1840–1841.
 (39) Kato, H. S.; Noh, J.; Hara, M.; Kawai, M. *J. Phys. Chem. B* **2002**, *106*, 9655–9658.

attachment to gold. However, it cannot be ruled out that these separate vibrations arise from the molecular modes predicted at 153 and 308 cm^{-1} which possess a non-negligible IETS intensity and caused by large amplitude combinations of C–C–C bending and CH_2 twisting motions, respectively. We are currently performing additional experiments in order to conclusively identify the origin of these lowest-energy modes.

We next compare the IETS “fingerprint region” of a C-10 alkanethiolate SAM with that of a DOA-DTC monolayer. This region contains a number of modes which are very sensitive to the molecular tilt and packing structure adopted by a SAM. In Figure 4, a and b show IETS from 50 to 200 mV where our spectra display several characteristic modes useful for differentiating these monolayers. The most prominent difference is the intense peak at 87 mV (702 cm^{-1}) which is observed in the C-10 alkanethiolate (Figure 4a) but absent in the dithiocarbamate spectrum (Figure 4b). This peak coincides with a strong $\nu(\text{C}-\text{S})$ stretching vibration arising from molecules orientated perpendicular to the electrode surface. In this arrangement alkanethiolate molecules incorporate a $\nu(\text{C}-\text{S})$ mode parallel with the tunneling pathway which promotes efficient coupling of the vibration with electrons.^{32,33} This mode is not expected in dithiocarbamate IET spectra since the dual C–S bonds of the N–C–S₂ group lie within the plane of delocalized bonding, giving the analogous DTC bonds aromatic character. Instead, all DTC spectra display a characteristic mode at 71 mV which corresponds to the distinct ν_{II} vibration of the N–C–S₂ group discussed above. The remaining peaks displayed by both alkanethiolate and alkyl-DTC monolayers between 100 and 200 mV arise from previously described molecular vibrations of hydrocarbon chains.^{20,23,32,33} These modes are nearly identical in the alkanethiolate and DTC monolayers and arise from multiple CH_2 bending, $\nu(\text{C}-\text{C})$, and $\nu(\text{C}-\text{N})$ stretching vibrations. One noted difference however, is the much higher intensity observed for the DTC $\delta_{\text{s}}(\text{CH}_2)$ scissoring mode observed at 176 mV (1420 cm^{-1}) not found in the alkanethiolate IETS, which is instead dominated by intense $\gamma_{\text{w}}(\text{CH}_2)$ wagging peaks at slightly lower frequency. The greater importance of scissoring modes in DTC tunnel junctions is probably related to the orientation of the dual hydrocarbon substituents which can form smaller angles with the electrode surface.²⁵ In this geometry unique to dithiocarbamate SAMs, tunneling is more likely through the CH_2 units where scissoring modes take on a more dominant role.

In order to verify the unique orientation of the alkyl fragments in DTC SAMs, we performed infrared specular reflectance spectroscopy on a DDA-DTC monolayer bound to gold (see Supporting Information). The FT-IR spectra of the CH_2 stretching region revealed $\nu_{\text{as}}(\text{CH}_2)$ (2922.7 cm^{-1}) and $\nu_{\text{s}}(\text{CH}_2)$ (2853.7 cm^{-1}) modes which are indicative of both crystalline and liquid-like states in the monolayer and are distinctly different from those found in alkanethiolate SAMs of similar length which show a greater crystallinity.⁴⁰ The surface IR analysis is consistent with a heterogeneous mixture of chain orientations at the monolayer surface which would present favorable tunneling pathways that bypass the terminal methyl group.²⁵ The activation of additional transport channels from decreased

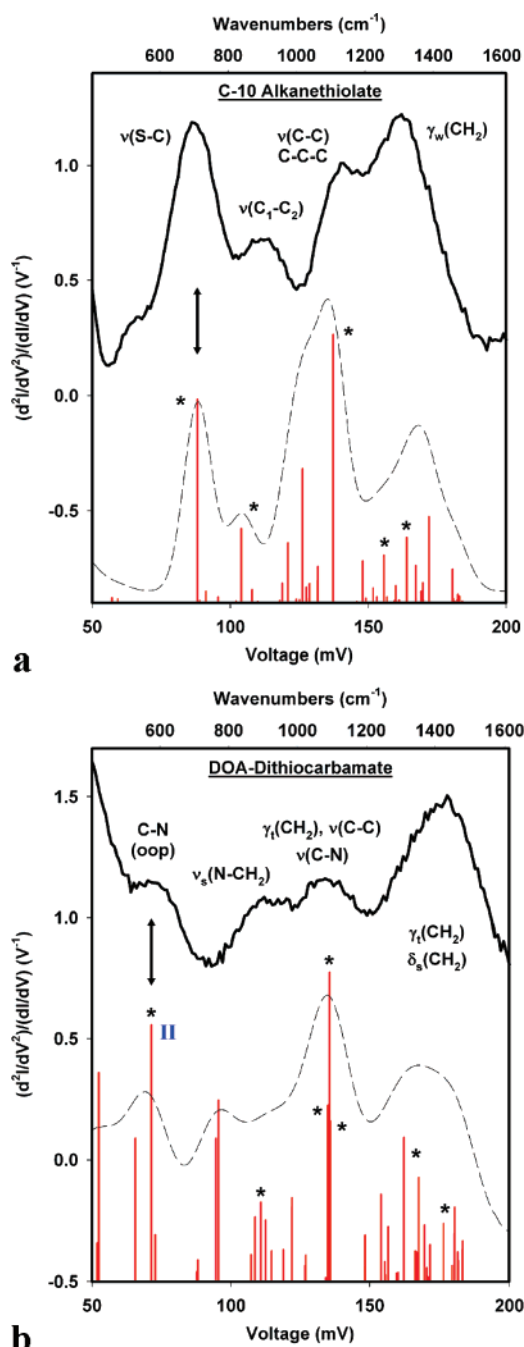


Figure 4. (a,b) Comparison of alkanethiolate and alkyl-dithiocarbamate IETS “fingerprint regions” from 50 to 200 mV bias. (a) IET spectra of a C-10 alkanethiolate monolayer on gold with calculated vibrational modes shown in red. (b) IET spectra of a DOA-DTC monolayer on gold. All spectra acquired using 6 mV modulation amplitude at 6 K and shown as the average of the forward and reverse traces. Asterisks mark calculated modes which coincide with dominant peaks observed in the experimental spectrum (black line). Dashed lines represent simulated spectra based on the calculated modes. Double-headed arrows mark the most characteristic peak for each monolayer system.

order within the film could result in prominent DTC $\delta_{\text{s}}(\text{CH}_2)$ scissoring modes observed in IETS. The peculiar orientation of the alkyl fragments in DTC SAMs is further supported by recent STM analysis which described a unique arrangement to the films. Alkanethiolate SAMs are known to adopt the characteristic $(\sqrt{3} \times \sqrt{3})R30^\circ$ packing structure while STM of analogous dialkyl-DTC monolayers revealed a hexagonal 2D arrangement with an unusually large lattice spacing compatible

(40) Weinstein, R.; Richards, J.; Thai, S. D.; Omiatsek, D. M.; Bessel, C. A.; Faulkner, C. J.; Othman, S.; Jennings, G. K. *Langmuir* **2007**, *23*, 2887–2891.

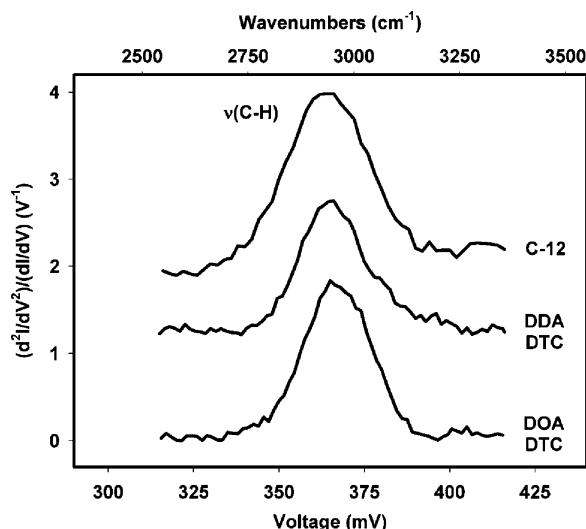


Figure 5. Comparison of alkanethiolate and dithiocarbamate $\nu(\text{C-H})$ stretching modes. IETS from 315 to 415 mV comparing C-12, DDA-DTC, and DOA-DTC self-assembled monolayers.

with the larger tilting of the DTC substituents.¹² Determining the role dithiocarbamate substituent angle has in the overall transport properties of the monolayer is beyond the capabilities of the microsphere test bed and will require additional analytical tools to fully determine its effect. However, the sensitivity of IETS to changing transport pathways suggests the differences in chain orientation within DTC monolayers is altering the manner in which electrons tunnel through the film, giving rise to prominent scissoring modes not observed in alkanethiolate monolayers.

One mode found to be common to both monolayer systems is the intense $\nu(\text{C-H})$ stretching vibration observed at approximately 364 mV (2936 cm^{-1}) and shown in Figure 5. As expected, no change is observed in this peak when comparing our monolayers using IETS, confirming that the use of different attachment chemistry has no effect on the “terminal” mode at the nonbonding CH_3/Au interface. However, all of our alkyl-monolayers display an unusually intense C-H mode relative to the peaks in the fingerprint region (Figure 2b), suggesting the signal does not arise exclusively from the terminal methyl group of the alkyl monolayer. Recent IETS experiments have demonstrated that extensive substitution of hydrogen atoms with fluorine in alkanethiolate tunnel junctions results in little modulation of the $\nu(\text{C-H})$ stretching mode as is normally found in IR and Raman spectroscopies.⁴¹ It was postulated that this effect may be due to a preference of inelastic electron tunneling interactions for methylene vibrations adjacent to the chemical attachment at the electrode (Au-S) rather than those near a nonbonding CH_3/Au interface. Although the disorder in alkyl-DTC SAMs discussed above may explain this effect for the dithiocarbamate system, we also observe a similar effect in IETS of alkanethiolate monolayers. Another possible cause for this intense mode may be film compression during junction fabrication. During fabrication of our devices, magnetic entrapment of the microspheres is expected to cause monolayer compression which would induce tilting of the molecules and possible activation of C-H stretching modes along the alkyl chains. This

would lead to activation of methylene units near the electrode surface and an intense $\nu(\text{C-H})$ stretching mode, depending on the induced molecular tilt. All tunnel junctions whose fabrication creates compression of the SAM may be susceptible to this effect. Although subtle, such influences on the transport properties of molecules within different nanoscale architectures must be understood in order to create viable molecular electronic devices.

Variation in microsphere contact area caused by the magnetic assembly process limited our analysis of alkyl-dithiocarbamate transport behavior to techniques which are independent of junction size (number of molecules in a device).²³ IETS, for example, has been shown to yield identical molecular spectra using test structures which differ widely in architecture and junction area.^{20,23} Although our technique precludes a quantitative assessment of DTC charge density, we were able to perform a qualitative comparison of multiple devices incorporating both alkyl-DTC and alkanethiolate monolayers. This comparison revealed DTC monolayers are consistently more conductive than alkanethiolate SAMs of similar length by a factor of 20 (± 4) at 200 mV bias (see Supporting Information). The observed increase is in good agreement with recent calculations which predicted a stronger coupling of the DTC π -conjugated system to the surface of gold will enhance electrical conductance through the monolayer by a factor of 25 at 1 V bias.¹⁵ Although a comparison of our devices displays the expected increase in molecular conductivity, additional analysis will be needed to determine to what extent the observed increase is actually caused by improved orbital overlap between the DTC moiety and metal binding sites. Known structural differences between alkyl-dithiocarbamate and alkanethiolate monolayers could also give rise to an enhancement of junction conductivity unrelated to the DTC attachment if a substantial portion of charge carriers were using an alternate path or “shortcut” through the molecules which bypass the terminal methyl group. It has been noted how the increased importance of IETS scissoring modes in alkyl-DTC tunnel junctions appears related to the unusual tilt angle of the dual hydrocarbon substituents. In addition, surface-IR analysis of alkyl-DTC monolayers confirms the hydrocarbon chains exist in a partially liquid-like state which presents a heterogeneous alkyl surface to the top metal contact (microsphere) in our devices. Other differences between alkyl-dithiocarbamate and alkanethiolate SAMs, such as monolayer packing structure and molecular surface density,¹² could also affect current density and will need to be examined further in order to determine the true link between dithiocarbamate attachment chemistry and molecular conductivity.

To conclude, we have compared the IETS characteristics of alkyl monolayers which utilize dithiocarbamate and thiolate attachments to gold. IETS is shown to be a valuable method for the characterization and differentiation of monolayers which differ by their method of covalent attachment to metal surfaces. IET spectra from both monolayer systems exhibit similar vibronic contributions arising from their hydrocarbon substituents, displaying a propensity for longitudinal modes parallel with the alkyl chains of the molecules. The appearance of distinct IETS modes from the dithiocarbamate moiety confirms electron transport through the delocalized orbitals of the bidentate structure. IETS also reveals that tunneling electrons couple strongly to molecular motions of the group binding the

(41) Beebe, J. M.; Moore, H. J.; Lee, T. R.; Kushmerick, J. G. *Nano Lett.* **2007**, *7*, 1364–1368.

molecules to the electrode surface, yielding characteristic peaks for each method of attachment and useful for identification. In addition, subtle differences in the IETS of these monolayers suggest the unique packing structure and organization of the dual hydrocarbon chains in alkyl-dithiocarbamate SAMs are influencing the transport properties through the DTC molecules. We are currently applying these techniques to further understand electron transport in additional chemical attachments to gold.

Acknowledgment. We gratefully acknowledge financial support from the Defense Advanced Research Project Agency

(DARPA). A.T. is grateful to the Royal Society of Chemistry (U.K.) for support.

Supporting Information Available: Additional IETS and $I(V)$ comparisons of alkanethiolate and alkyl-dithiocarbamate SAMs, movies illustrating DTC modes I and II, FT-IR specular reflectance data, and additional computational details. This material is available free of charge via the Internet at <http://pubs.acs.org>.

JA074970Z